DMD Fast Forward. Published on March 27, 2008 as doi:10.1124/dmd.107.020248

The Biotransformation of Prasugrel, a New Thienopyridine Prodrug, by the Human Carboxylesterases 1 and 2

Eric T. Williams
Karen O. Jones
G. Douglas Ponsler
Shane M. Lowery
Everett J. Perkins
Steven A. Wrighton
Kenneth J. Ruterbories
Miho Kazui
Nagy A. Farid

Department of Drug Disposition [ETW, GDP, SML, EJP, SAW, KJR, NAF] and Pharmaceutical Research Development [KOJ], Lilly Research Laboratories, Eli Lilly and Company, Indianapolis, IN 46285, USA; Drug Metabolism and Pharmacokinetics Research Labs, Daiichi Sankyo, Company, Limited, Tokyo, Japan [MK]

Running Title:
Prasugrel Biotransformation by the Human Carboxylesterases

Corresponding Author:
Nagy A. Farid
Eli Lilly and Company
Lilly Research Laboratories
Drop Code 0714
Indianapolis, IN 46285

Text Pages: 18
Tables: 0
Figures: 3
References: 28
Abstract: 246
Introduction: 639
Discussion: 1655

Abbreviations:
hCE1 – human carboxylesterase 1; liver-dominant form
hCE2 – human carboxylesterase 2; intestinal-dominant form
CL_{int} – intrinsic clearance
IC_{50} – half the maximal inhibitory concentration
K_m – concentration at half of V_{max}; Michaelis-Menten constant
V_{max} – maximum velocity
Prasugrel – 2-acetoxy-5-(α-cyclopropylcarbonyl-2-fluorobenzyl)-4,5,6,7-tetrahydrothieno[3,2-c]pyridine
R-95913 – 2-[2-oxo-6,7-dihydrothieno[3,2-c]pyridin-5(4*H*)-yl]-1-cyclopropyl-2-(2-fluorophenyl)ethanone
R-138727 – 2-[1-[2-cyclopropyl-1-(2-fluorophenyl)-2-oxoethyl]-4-mercapto-3-piperidinylidene]acetic acid

DMD Fast Forward. Published on March 27, 2008 as DOI: 10.1124/dmd.107.020248
This article has not been copyedited and formatted. The final version may differ from this version.

Prasugrel is a novel thienopyridine prodrug with demonstrated inhibition of platelet aggregation and activation. The biotransformation of prasugrel to its active metabolite, R-138727, requires ester bond hydrolysis, forming the thiolactone R-95913, followed by cytochrome P450-mediated metabolism to the active metabolite. The presumed role of the human liver- and intestinal-dominant carboxylesterases, hCE1 and hCE2, respectively, in the conversion of prasugrel to R-95913 was determined using expressed and purified enzymes. The hydrolysis of prasugrel is at least 25-times greater with hCE2 than hCE1. Hydrolysis of prasugrel by hCE1 demonstrated Michaelis-Menten kinetics yielding an apparent K_m of 9.25 μM and an apparent V_{max} of 0.725 nmol of product/min/μg of protein. Hydrolysis of prasugrel by hCE2 showed a mixture of Hill kinetics at low substrate concentrations and substrate inhibition at high concentrations. At low concentrations, prasugrel hydrolysis by hCE2 yielded an apparent K_s of 11.1 μM, an apparent V_{max} of 19.0 nmol/min/μg, and an apparent Hill coefficient of 1.42; while at high concentrations, an apparent IC_{50} of 76.5 μM was obtained. In humans, no *in vivo* evidence of inhibition exists. *In vitro* transport studies using the intestinal Caco-2 epithelial cell model demonstrated a high *in vivo* absorption potential for prasugrel and rapid conversion to R-95913. In conclusion, the human carboxylesterases efficiently mediate the conversion of prasugrel to R-95913. These data help explain the rapid appearance of R-138727 in human plasma, where maximum concentrations are observed 0.5 hour after a prasugrel oral dose, and the rapid onset of action of prasugrel.

Platelet aggregation and activation is a serious concern for patients who undergo percutaneous coronary intervention and stent placement. The underlying mechanism of platelet aggregation is mediated through two G-protein coupled P2 receptors, $P2Y_1$ and $P2Y_{12}$ (Gachet, 2001). $P2Y_1$ activation leads to a transient aggregation, while $P2Y_{12}$ activation maintains a sustained aggregation. To reduce platelet aggregation, the development of $P2Y_{12}$ selective inhibitors has yielded the thienopyridine prodrugs, which include ticlopidine, clopidogrel (structures available in Farid *et al.*, 2008), and prasugrel (Figure 1), a novel thienopyridine currently in clinical development.

While the active metabolites for prasugrel and clopidogrel have equipotency at the $P2Y_{12}$ receptor *in vitro* (Sugidachi *et al.*, 2007), orally administered prasugrel is 10 and 100 times more effective on an equal dose basis in inhibiting platelet aggregation than clopidogrel and ticlopidine, respectively (Niitsu *et al.*, 2005). Clopidogrel and prasugrel differ markedly in the biotransformation pathways leading to their activation. Prasugrel (Figure 1) has a single dominant metabolic pathway leading to the active metabolite (Farid *et al.*, 2007a). However, clopidogrel has two competing metabolic pathways for the parent compound, with the major pathway leading to the formation of an inactive metabolite, clopidogrel carboxylic acid derivative (Caplain *et al.*, 1999). The clopidogrel carboxylic acid derivative is formed through ester hydrolysis by the human carboxylesterase (hCE) 1 (Tang *et al.*, 2006). The minor pathway in clopidogrel metabolism yielding the active metabolite requires two sequential steps of cytochrome P450 (CYP) biotransformation (Kurihara *et al.*, 2005). Whereas, prasugrel bioactivation requires the hydrolysis of the ester then oxidation of the formed thiolactone, R-95913 (Farid *et al.*, 2007a) (Figure 1) to form the active metabolite of prasugrel. The oxidation

of R-95913 has been shown to be mediated by several CYP enzymes, but primarily by CYP3A and CYP2B6 (Rehmel *et al.*, 2006).

The carboxylesterases are a multigene family that hydrolyze compounds containing an ester, amide, or thioester linkage. Carboxylesterases are broadly expressed throughout the body with two major forms in humans, hCE1 and hCE2. Although both forms have high mRNA expression in the liver, hCE1 levels exceed those of hCE2 (Satoh *et al.*, 2002). Importantly, the extrahepatic expression differs between hCE1 and hCE2 (Satoh *et al.*, 2002). For hCE1, the liver-dominant form, extrahepatic mRNA expression observed in decreasing order are the stomach, testis, kidney, spleen, and colon. The intestinal-dominant form, hCE2, has extrahepatic mRNA expression in decreasing order in the colon, small intestine, and heart. In addition to the studies examining mRNA expression, the relative activity of the two enzymes has been recently demonstrated in the liver and small intestine (Imai *et al.*, 2006). Using tissue preparations, hCE1 and hCE2 were separated in non-denaturing gels, and the hydrolysis of 1-naphthylbutyrate was utilized to determine the relative activity of the two enzymes. Both enzymes were detected in the liver, but hCE1 was clearly the dominant form. Unlike the liver, the small intestine demonstrated that hCE2 was the dominant form with a minor contribution by hCE1. This pattern of tissue distribution has been further demonstrated (Taketani *et al.*, 2007).

Although hCE1 and hCE2 have overlapping substrate recognition, clear evidence of ester-based substrate specificity has been observed (Satoh *et al.*, 2002). Two products result from ester hydrolysis, an alcohol and an acyl moiety. In general, hCE1 prefers substrates with a large acyl moiety, while hCE2 prefers substrates with a large alcohol substituent. Based upon this substrate-activity relationship, prasugrel would be predicted to be a preferred substrate for hCE2.

This study aims to investigate the role of hCE1 and hCE2, the dominant forms in the liver and intestinal tract, respectively, in the bioactivation of prasugrel. To accomplish this endeavor, hCE1 and hCE2 enzymes were expressed and purified and used to determine the formation kinetics of R-95913 from prasugrel. Additional experiments were conducted with Caco-2 monolayers to assess the conversion of prasugrel to R-95913 and their relative transit across this intestinal model.

In Vitro Hydrolysis Assays

For the hydrolysis assays, each reaction tube contained buffer, enzyme, prasugrel, and acetonitrile, in a total volume of 600 µL. The buffer used was Dulbecco's Phosphate Buffered Saline (D-PBS; 14040-117; Invitrogen, Corp.; Carlsbad, CA). A 5 mM stock of prasugrel was prepared in acetonitrile. The final reaction volume contained a total of 2% acetonitrile. Prasugrel concentrations used with hCE1 were 0.855, 1.71, 3.42, 6.84, 13.7, 27.4, 54.7, and 109 µM. In addition to the concentrations used with hCE1, the hCE2 studies also used 21.9, 40.5, 71.2, and 87.6 µM. The expression and purification of hCE1 and hCE2 were previously described (Williams *et al.*, 2008). All protein preparations are homogenous based upon analysis of an SDS-PAGE gel stained with SimplyBlue SafeStain (Invitrogen, Corp.; data not shown). The tubes containing the various prasugrel concentrations were pre-incubated in a water bath at 37°C for approximately 1 minute. The enzyme, either 1 µg/mL of hCE1 or 0.25 µg/mL of hCE2, was pre-incubated with buffer for approximately 5 minutes at 37°C and added to the tubes with prasugrel to start the reaction. A 100 µL aliquot was removed from the reaction tube at 1, 2, 3, and 6 minutes after reaction initiation then a 100 µL of acetonitrile containing 2 µg/mL of a d_4-labeled R-95913 as the internal standard was added to each aliquot to terminate the reaction. All studies were conducted in triplicate.

For the standards, a stock solution of R-95913 was prepared in acetonitrile at 2 mg/mL. The concentrations ranged from 4.88 ng/mL to 40 µg/mL, in 2% acetonitrile in D-PBS. Each standard (100 µL) was added to 100 µL of acetonitrile with internal standard. In addition to the standards, two blanks were also included. One blank was lacking R-95913, but included the internal standard. The second blank was lacking both R-95913 and internal standard. Samples and standards had two dilution schemes for analysis, 1:25 and 1:275 dilution, with the diluent

being methanol:water (1:1, v:v). The appropriate dilution was utilized for analysis to ensure samples did not saturate the detector response of the mass spectrometer.

Study samples were analyzed by LC-MS/MS using a Sciex API 4000 triple quadrupole mass spectrometer (Applied Biosystems/MDS; Foster City, CA) equipped with a TurboIonSpray interface, and operated in positive ion mode. The analytes were chromatographically separated using a Betasil C_{18} 2.1x20 mm, 5 µm, Javelin HPLC column (Thermo Fisher Scientific, Inc.; Waltham, MA), with a gradient LC system composed of water:1 M ammonium bicarbonate, (200:1, v:v) (Mobile Phase A), and methanol:1 M ammonium bicarbonate, (200:1, v:v) (Mobile Phase B). The pumps were a Shimadzu LC-10AD with a SCL-10A controller (Kyoto, Japan). Also, a Gilson 215 liquid handler (Middleton, WI) was used. The gradient profile changed from 30% B at 0 min, 42% B at 0.01 min to 0.10 min, 75% B at 0.20 to 0.30 min, and 98% at 0.31 to 0.76 min, at a flow rate of 1.5 mL/min. Chromatography was performed at ambient temperature, with 1 mL/min directed to the mass spectrometer between 0.18 and 0.5 min (0.5 mL/min split to waste). Selected reaction monitoring $(M+H)^+$ transitions m/z 332.2 > 177.1 and 336.2 > 149.2 were monitored for R-95913, and the internal standard, respectively. The TurboIonSpray temperature was maintained at 725ºC, with collision, curtain, nebulizing, and desolvation gas (nitrogen) settings of 8, 10, 50, and 70, respectively. The ionspray voltage was set to 4000 V, while the respective declustering, entrance, collision, and exit potentials were 55, 10, 27, and 4 for R-95913, and 55, 10, 33, and 8 for the internal standard. The mass spectrometer quadrupoles were tuned to achieve unit resolution (0.7 DA at 50% FWHM). Data were acquired and processed with Analyst 1.4.1 (Applied Biosystems).

For the assays with hCE1, the standards for the 1:25 dilution ranged from 19.5 to 2500 ng/mL. A correlation coefficient of 0.999 was achieved with less than a 7% deviation from the

relative mean using a quadratic curve with a weighting of $1/X^2$. The standards for the 1:275 dilution ranged from 156 to 20000 ng/mL. A correlation coefficient of 0.998 was achieved with less than a 12% deviation from the relative mean using a quadratic curve with a weighting of $1/X^2$. For the assays with hCE2, the standards for the 1:25 dilution ranged from 78.1 to 2500 ng/mL. A correlation coefficient of 0.998 was achieved with less than a 9% deviation from the relative mean using a quadratic curve with a weighting of $1/X^2$. The standards for the 1:275 dilution ranged from 625 to 10000 ng/mL. A correlation coefficient of 0.999 was achieved with less than a 6% deviation from the relative mean using a quadratic curve with a weighting of $1/X^2$.

Enzyme Kinetic Modeling

Hydrolysis reaction rates (nmol of product/min/µg of protein) were calculated from the linear portion of the product concentration versus time curve. Fitting the rate data to standard kinetic models (Copeland, 1996) was accomplished using WinNonlin (Pharsight Corp.; Mountain View, CA). Michaelis-Menten, substrate inhibition, and Hill kinetic models with differing weighting were used. For the results with hCE1, Michaelis-Menten kinetics using a weighting of $1/Y^2$ provided the best fit. However, the unusual kinetics of the formation of R-95913 by hCE2 could not be fit to the models described above as demonstrated by the standard errors of the fit being large as compared to the kinetic values. Therefore, the product formation rate data obtained with incubation with hCE2 between 0.855 and 40.5 µM of prasugrel were found to best fit the Hill model using a weighting of $1/\hat{Y}^2$. The rate data with hCE2 and prasugrel concentrations between 27.4 and 109 µM were fit to an IC_{50} model using Prism (GraphPad Software, Inc.; San Diego, CA). The various estimated parameters are reported as the value ± the standard error of the estimate.

Intestinal Transport and Metabolism Assays

The Caco-2 cell line was obtained from the American Type Culture Collection (ATCC; Rockville, MD) and grown under standard culture conditions of 37ºC in a humidified atmosphere containing 5% CO_2. Caco-2 cell monolayers were cultured in 175 cm^2 flasks in Dulbecco's Modified Eagle Medium (DMEM; 12430-054; Invitrogen, Corp.) supplemented with 10% fetal bovine serum (FB-01; Omega Scientific, Inc.; Tarzana, CA), 1 mM sodium pyruvate (25-000-CI; Mediatech, Inc.; Herndon, VA), 100 mM non-essential amino acids (25-025-CI), 2 mM L-glutamine, 100 U/mL penicillin (30-002-CI), and 100 µg/mL streptomycin. Cells were seeded at a density of 60,000 cell/cm^2 onto collagen-coated 12-well Costar Transwell® polycarbonate membranes (0.4 µm pore size, 1.13 cm^2 surface area) and used between 21 to 28 days post-seeding. The culture medium was changed every other day for 10 days after seeding onto Transwell® filters, and daily afterwards. Cells of passage number 61 were used for these studies.

Studies were performed with Hank's Balanced Salt Solution (14065-056; Invitrogen, Inc.) containing 10 mM HEPES (15630-080) and 15 mM glucose (G-5400; Sigma-Aldrich, Corp.; St. Louis, MO), pH 7.4 (HBSS+) at 37ºC with 5% CO_2 in a humidified incubator. At the start of the experiment, monolayers were rinsed twice with HBSS+ and the transepithelial electrical resistance (TEER) of each cell monolayer was measured using an Endohm-12 resistence meter. Monolayers having TEER values outside the range of 450-650 $\Omega \cdot cm^2$ were discarded. Volumes in the apical and basolateral chambers were 0.5 mL and 1.5 mL, respectively. All studies were conducted in triplicate.

The apical-to-basolateral studies used an apical dosing solution of 5 µM prasugrel along with reference compounds, 100 µM atenolol (A-7655; Sigma-Aldrich, Corp.) and 10 µM

pindolol (P-0778; Sigma-Aldrich, Corp.). At each sampling time (0, 15, 30, 60, 90, and 120 minutes), a 200 µL aliquot of drug solution was removed from the basolateral receiver chamber and immediately replaced with an equal volume of drug-free buffer. Similarly, a 20 µL aliquot was removed from the apical donor chamber without replenishing the donor solution.

Monolayers were dosed with 0.5 mM Lucifer Yellow (L-453; Invitrogen, Inc.) to determine post-experimental monolayer integrity. Lucifer yellow was measured with a BMG Fluostar 403 microplate reader using an excitation wavelength of 485 nm and an emission wavelength of 538 nm. Each determination was performed in triplicate and was not significantly greater than baseline.

The basolateral-to-apical studies used a basolateral dosing solution of 5 µM prasugrel along with reference compounds, 100 µM atenolol and 10 µM pindolol. At each sampling time (0, 15, 30, 60, 90, and 120 minutes), a 200 µL aliquot of drug solution was removed from the apical receiver chamber and immediately replaced with an equal volume of drug-free buffer. Similarly, a 20 µL aliquot was removed from the basolateral donor chamber without replenishing the donor solution. A post-experimental monolayer integrity check was conducted with Lucifer Yellow, as described above.

A 10 mM stock solution of prasugrel and R-95913 in DMSO was prepared. Further dilution in 1:1 ACN:water gave a 100 µM stock. Atenolol stocks (10 mM in water and 100 µM in 1:1 ACN:water) and pindolol stocks (10 mM in DMSO and 10 µM in 1:1 ACN:water) were prepared previously. Standard curves were obtained by serial dilution in 1% formic acid in ACN:Hanks buffer, pH 7.4 (1:1).

Caco-2 study samples were diluted in 1% formic acid in ACN:Hanks buffer, pH 7.4 (1:1), then analyzed by LC-MS/MS using a Sciex API 3000 triple quadrupole mass spectrometer

(Applied Biosystems/MDS) equipped with a TurboIonSpray interface, and operated in positive ion mode. The analytes were chromatographically separated using a BDS Hypersil C_{18} 30x2.1 mm 3 µm HPLC column (Thermo Fisher Scientific, Inc.). The buffer consisted of 25 mM NH_4OH, adjusted to pH 3.5 with 88% formic acid. The gradient LC system composed of 10% buffer in water (Mobile Phase A) and 10% buffer in acetonitrile (Mobile Phase B). Rheos 2000 micropumps (Thermo Fisher Scientific, Inc.) and CTC Analytics HTC PAL autosampler (Zwingen, Switzerland) were used. The mobile phase composition changed from 0% B at 0 min, 100% B at 0.02 min to 1.00 min, 100% B at 1.00 to 2.50 min, 0% at 2.50 to 2.60 min, and 0% from 2.60 to 4.00 min, at a flow rate of 0.3 mL/min. Chromatography was performed at ambient temperature. Selected reaction monitoring $(M+H)^+$ transitions m/z 374.0 > 206.1, 332.2 > 109.3, 267.2 > 145.0, and 249.0 > 116.2 were monitored for prasugrel, R-95913, atenolol, and pindolol, respectively. The TurboIonSpray temperature was maintained at 450ºC, with collision, curtain, and nebulizer gas settings of 10, 10, and 8, respectively. The ionspray voltage was set to 5000 V, while the respective declustering, focusing, entrance, collision, and exit potentials were 46, 200, 10, 35, and 12 for prasugrel, 31, 150, 10, 50, and 10 for R-95913, 36, 170, 10, 35, and 8 for atenolol, and 36, 170, 10, 35, and 6 for pindolol.

The standards for prasugrel, R-95913, pindolol, and atenolol ranged from 10 to 1000 nM. For prasugrel and R-95913, the correlation coefficients were 1.00 and 1.00, respectively, with a maximum deviation of 3% and 4%, respectively, from the relative mean using a quadratic curve with a weighting of $1/X^2$. For pindolol and atenolol, the correlation coefficients were 0.998 and 0.999, respectively, with a maximum deviation of 8.8% and 10%, respectively, from the relative mean using a linear curve with a weighting of $1/X^2$.

The formation and disappearance rates of prasugrel and R-95913 were calculated using Microsoft Excel. The rates (nmol/hr) are the result of using the SLOPE function with data points in the linear range, as described in the results section.

The human carboxylesterases hCE1 and hCE2 efficiently hydrolyzed prasugrel to R-95913, as shown in Figure 2. Figure 2A depicts the fit of standard Michaelis-Menten kinetics to the rate data for hCE1, which yields an apparent K_m of 9.25 ± 0.78 µM and an apparent V_{max} of 0.725 ± 0.035 nmol of product/min/µg of protein. However, the results obtained using hCE2 (Figure 2B) were determined to fit poorly to all standard enzyme kinetic models, including that for substrate inhibition. Therefore, the results obtained with hCE2 were divided into two data sets for modeling. The first data set consisted of the results between prasugrel concentrations of 0.855 and 40.5 µM to model for standard enzyme kinetics. The best fit with this data set was produced using the Hill equation, which gave an apparent K_s of 11.1 ± 2.8 µM, an apparent V_{max} of 19.0 ± 2.8 nmol of product/min/µg of protein, and an apparent Hill coefficient (N) of 1.42 ± 0.12. The second portion of the curve resembles an inhibition plot and as such the data between 27.4 and 109 µM was modeled for inhibition to yield an apparent IC_{50} of 76.5 ± 2.7 µM.

Due to the different models needed to fully describe the diverse kinetics observed, the clearance near the therapeutic concentration range (Williams *et al.*, 2002) was also compared. The clearance by each enzyme was calculated using the substrate concentrations between 0 and 14 µM, which resulted in a linear slope of 32 µL/min/µg and 798 µL/min/µg for hCE1 and hCE2, respectively, yielding R^2 values of 0.955 and 0.938, respectively. This comparison indicates that the rate of hydrolysis of prasugrel at low substrate concentrations is about 25-times greater for hCE2 than hCE1.

The Caco-2 monolayer transport and metabolism study demonstrated the conversion of prasugrel to R-95913 (Figure 3). The active metabolite of prasugrel, R-138727, was not monitored since CYP3A4, which is the primary CYP involved in its formation from the thiolactone, R-95913, (Rehmel *et al.*, 2006), is not routinely expressed in Caco-2 monolayers

(Cummins *et al.*, 2004). Figures 3A and B show the apical to basolateral (representing lumen to blood) conversion and transport of the cumulative amounts of prasugrel and R-95913 in the donor and receiver compartments, respectively. As shown in Figure 3A, the appearance rate of R-95913 in the donor (apical) buffer is 1.65 ± 0.40 nmol/hr between 0 and 30 minutes, and the loss of prasugrel between 0 and 30 minutes occurs at a rate of 2.80 ± 0.34 nmol/hr. For Figure 3B, the appearance rate of R-95913 in the receiver (basolateral) buffer is 0.730 ± 0.028 nmol/hr between 0 and 90 minutes, and prasugrel was not detected. Similarly, Figures 3C and D show the basolateral to apical (representing blood to lumen) prasugrel conversion and transport. Figure 3C demonstrates a loss of prasugrel in the donor (basolateral) buffer at a rate of 1.98 ± 0.10 nmol/hr between 30 and 120 minutes, and the appearance rate of R-95913 between 0 and 90 minutes is 1.41 ± 0.08 nmol/hr. In Figure 3D, the appearance rate for R-95913 in the receiver (apical) buffer is 0.510 ± 0.043 nmol/hr between 0 and 90 minutes, and prasugrel was not detected.

These studies demonstrate that both hCE1 and hCE2 have similar K_m and K_s values for the ester hydrolysis of prasugrel, suggesting they bind prasugrel with similar affinity. However, the rate of hydrolysis (V_{max}) by hCE2 appears to be 26-times higher than that of hCE1. Since the pattern of kinetics for the hydrolysis of prasugrel by hCE1 and hCE2 were found to be quite different, the hydrolysis rates at low substrate concentrations, as previously described (Williams *et al.* 2002), were used as a potentially more meaningful comparison. This comparison indicates the hydrolysis of prasugrel by hCE2 at low substrate concentrations is 25-times greater than that for hCE1. This pattern of substrate selectivity by CEs is consistent with published data (Satoh *et al.*, 2002). Upon hydrolysis of the ester, thioester, or amide bond, an alcohol and acyl moiety are released as metabolites. The relative sizes of these two moieties have been shown to predict which enzyme will have preferential recognition of the substrate (Satoh *et al.*, 2002). Substrates yielding a smaller alcohol moiety, such as clopidogrel (Tang *et al.*, 2006), are preferred by hCE1. However, hCE2 has a preference for substrates that yield a smaller acyl moiety upon hydrolysis, like prasugrel.

Prasugrel appears to have a higher binding affinity (lower K_m value) for the human CEs as compared to other characterized CE substrates. When compared to irinotecan (CPT-11), the binding affinity of prasugrel is about four-times greater for hCE1 but ten-times lower for hCE2 (Sanghani *et al.*, 2004). As compared to heroin, the binding of prasugrel to hCE1 and hCE2 is substantially greater, by about 600-times (Kamendulis *et al.*, 1996). Similar to heroin, the binding affinities of cocaine and 4-methylumbelliferyl acetate (Pindel *et al.*, 1997) are lower by at least ten-times for prasugrel with both enzymes. Also, when compared to 4-nitrophenyl butyrate the binding affinity of prasugrel is about ten-times greater (Williams *et al.*, 2008).

Therefore, prasugrel appears to have a higher binding affinity for the human CEs than most CE probe substrates.

For the hydrolysis of prasugrel by hCE2, the kinetic terms determined, K_s, V_{max}, and IC_{50}, are estimates of these descriptors because of the unusual shape of the kinetic curve. Due to the highly significant substrate inhibition observed, the reported V_{max} is likely underestimated. Thus, it is best described in this context as the maximum achievable velocity. Since the V_{max} is likely underestimated, the determined K_s and IC_{50} values may also be inaccurate. However, the observed values are relevant in the context of this system since the values reflect the maximal values possible using purified enzymes without other metabolic or clearance pathways involved.

The most unique feature of the prasugrel hydrolysis curve obtained with hCE2 is the steep inhibition phase that becomes apparent around the substrate concentration of 50 µM and results in nearly complete inhibition by 109 µM. Fitting the entire kinetic curve to the classical substrate inhibition model resulted in an extremely poor fit of the data at high substrate concentrations since the model does not accommodate nearly 100% inhibition. However, an enzyme kinetic model has been proposed to describe such results (Kühl, 1994). Kühl proposed that prior to the completion of the first catalytic cycle, an extended recovery period for the enzyme's active site could permit a side interaction with a second substrate molecule. This interaction would prevent the enzyme from returning to its initial state for a new reaction cycle until the second substrate molecule dissociates from the active site. Interestingly, this concept is consistent with the carboxylesterase reaction cycle, which involves the covalent binding of the acyl moiety of the substrate to the CE active site, followed by cleavage of the ester bond and the release of the alcohol moiety, then regeneration of the active enzyme by the release of the acyl moiety from the enzyme (Satoh and Hosokawa, 1998). In the case of hCE2 which has a

preference for a small acyl moiety, the initial substrate molecule would bind, and cleavage occur allowing the bulky alcohol moiety to vacate the active site. Before the regeneration of the enzyme active site by the removal of the small acyl moiety, a second substrate molecule could bind and prevent the enzyme from completing the catalytic cycle. This would prevent the new molecule from being hydrolyzed and result in the inhibition observed for hCE2. This hypothesis is consistent with the model proposed by Kühl and is the subject of future work.

Additional possible explanations for the inhibition observed for hCE2 at high substrate concentrations involve the potential for multiple substrate binding sites. The active site of CEs contain two binding pockets (Satoh *et al.*, 2002), and the entrance to the active site of hCE2 is less restrictive than hCE1 (Wadkins *et al.*, 2001). Thus, a potential explanation is that multiple molecules may interact with the active site of hCE2 resulting in the unproductive binding of substrates. Other than the active site itself, hCE2 may have an external binding site similar to the Z-site found with hCE1 that could affect catalysis. It is known that substrate binding to the Z-site of hCE1 results in conformational changes that alter enzyme activity (Bencharit *et al.*, 2003). Since a crystal structure does not yet exist for hCE2, it is unknown if it has a similar Z-site or can bind multiple substrate molecules.

Despite the apparent *in vitro* inhibition of hCE2 at high prasugrel concentrations, there is no evidence that this occurs *in vivo*. A linear relationship has been shown between the prasugrel dose (2.5 mg to 75 mg) and the plasma exposure (AUC) of R-95913 (Asai *et al.*, 2006). The micromolar equivalents of the 2.5, 10, and 75 mg doses of prasugrel dissolved in a standard glass of water (250 mL) would result in concentrations of 26.8, 107, and 803 µM, respectively. If the *in vitro* inhibition results were combined with these calculated intestinal lumen prasugrel concentrations and used to predict the *in vivo* inhibition, then hCE2 would not be substantially

inhibited with the 2.5 mg dose, but might be inhibited at the other doses. If such inhibition were to occur, this would result in a disproportionately higher exposure to R-95913 after a 2.5 mg dose compared to the higher doses, which has not been observed. Therefore, the observed *in vitro* hCE2 inhibition does not translate to *in vivo* relevance. The lack of observed *in vivo* inhibition could be due to the large intestinal surface area, thus intracellular hCE2 is not exposed to the high calculated intestinal concentrations of prasugrel. Also, hCE1 or other esterases may have sufficient capacity to compensate for a loss in hCE2 activity, if any.

The Caco-2 monolayer transport and metabolism study demonstrated efficient conversion of prasugrel to R-95913 (Figure 3). For both apical and basolateral administration, prasugrel is only found in the donor buffer and not the receiver buffer, which indicates that prasugrel does not pass through this intestinal model unmodified. Also, the loss of prasugrel, R-95913 formation, and R-95913 transit across the monolayer occur slightly faster when dosed on the apical versus the basolateral surface. While Caco-2 cells are not a perfect intestinal model system to study carboxylesterases due to the relatively high levels of hCE1 versus hCE2 (Imai *et al.*, 2005), the results obtained from these studies with prasugrel are consistent with the ideas presented when temocapril and 4-nitrophenyl acetate were used as substrates. In the study conducted by Imai *et al.*, the brush-border membrane vesicles (BBMV) of the Caco-2 cells were isolated from the remaining cellular S9 fraction. Temocapril, a substrate for hCE1, was hydrolyzed in the S9 fraction, but not as well in the BBMV; the generic esterase susbstrate 4-nitrophenyl acetate had much higher hydrolysis in the BBMV. Despite the presence of esterase activity in the BBMV, hCE1 is predominantly in the S9 fraction. Since the formation rate of R-95913 was similar whether dosed apically or basolaterally, S9 hydrolysis is suggested. The

slightly higher hydrolysis rate when prasugrel was dosed on the apical membrane could be due to the additional hydrolysis occurring in the BBMV.

The results of the Caco-2 studies are in agreement with the data obtained in humans where prasugrel was found to be rapidly absorbed and metabolized and was not detected in plasma (Farid *et al.*, 2007b). In addition, prasugrel and its hydrolysis product, R-95913, were not detected in human feces, but only metabolites of these two compounds were found in the feces. The above data suggest that after an oral dose, prasugrel was essentially fully absorbed and metabolized before excretion (Farid *et al.*, 2007b). However, a role for other enzymes or intestinal microflora in the metabolism of prasugrel cannot be precluded.

Conclusion

Both hCE1 and hCE2 appear to have similar binding affinities ($K_{m/s} \approx 10$ µM) for prasugrel, but hCE2 has about a 26-times greater maximal hydrolysis rate (V_{max} = 19.0 nmol of R-95913/min/µg of protein) than hCE1 (V_{max} = 0.725 nmol of R-95913/min/µg of protein). Further, the initial formation of R-95913 at low prasugrel concentrations is about 25-times higher with hCE2 (798 µL/min/µg) than hCE1 (32 µL/min/µg). Thus, although both hCE1 and hCE2 are capable of hydrolyzing prasugrel to R-95913, hCE2 appears to be the more efficient carboxylesterase for this conversion. Based upon these results, it is proposed that the biotransformation of prasugrel to R-95913 is mediated efficiently by hCE2, the dominant carboxylesterase in the intestine, prior to reaching the portal vein. Any remaining parent compound would likely be hydrolyzed by hepatic esterases. The results of the human carboxylesterase *in vitro* metabolism assays and the Caco-2 monolayer metabolism and transport studies, coupled with the fact that CYP3A accounts for ~80% of the total CYP content in the human small intestine (Paine *et al.*, 2006) help explain the rapid formation of the active

metabolite of prasugrel, R-138727, in humans, where maximum concentrations of R-138727 are observed 30 minutes after a prasugrel oral dose, and also the rapid onset of the inhibition of platelet aggregation by prasugrel (Farid *et al.*, 2007b, Brandt *et al.*, 2007).

The authors thank Barbara Ring, Eli Lilly and Company, for her thoughtful discussion of the work.

Asai F, Jakubowski JA, Naganuma H, Brandt JT, Matsushima N, Hirota T, Freestone S, Winters KJ (2006) Platelet inhibitory activity and pharmacokinetics of prasugrel (CS-747) a novel thienopyridine P2Y12 inhibitor: a single ascending dose study in healthy humans. *Platelets* **17**: 209-217.

Bencharit S, Morton CL, Xue Y, Potter PM, Redinbo MR (2003) Structural basis of heroin and cocaine metabolism by a promiscuous human drug-processing enzyme. *Nat Struct Biol* **10**: 349-356.

Brandt JT, Payne CD, Wiviott SD, Weerakkody G, Farid NA, Small DS, Jakubowski JA, Naganuma H, Winters KJ (2007) A comparison of prasugrel and clopidogrel loading doses on platelet function: magnitude of platelet inhibition is related to active metabolite formation. *Am Heart J* **153**: 66.e9-66.e16.

Caplain H, Donat F, Gaud C, Necciari J (1999) Pharmacokinetics of clopidogrel. *Semin Thromb Hemost* **25 (Suppl 2)**: 25-28.

Copeland RA (1996) *Enzymes: A Practical Introduction to Structure, Mechanism, and Data Analysis*. Wiley-VCH, New York.

Cummins CL, Jacobsen W, Christians U, Benet LZ (2004) CYP3A4-Transfected Caco-2 Cells as a Tool for Understanding Biochemical Absorption Barriers: Studies with Sirolimus and Midazolam. *J Pharmacol Exp Ther* **308**: 143-155.

Farid NA, McIntosh M, Garofolo F, Wong E, Shwajch A, Kennedy M, Young M, Sarkar P, Kawabata K, Takahashi M, and Pang H (2007a) Determination of the active and inactive metabolites of prasugrel in human plasma by liquid chromatography/tandem mass spectrometry. *Rapid Commun Mass Spectrom* **21**: 169-179.

Farid NA, Smith RL, Gillespie TA, Rash TJ, Blair PE, Kurihara A, Goldberg MJ (2007b) The

Disposition of Prasugrel, a Novel Thienopyridine, in Humans. *Drug Metab Disp* **35**: 1096-1104.

Farid NA, Payne CD, Ernest CS II, Li YG, Winters KJ, Salazar DE, and Small DS. (2008) Prasugrel, a new thienopyridine antiplatelet drug, weakly inhibits cytochrome P450 2B6 in humans. *J. Clin. Pharmacol*. **48**: 53-59

Gachet C (2001) ADP receptors of platelets and their inhibition. *Thromb Haemost* **86**: 222-232.

Imai T, Imoto M, Sakamoto H, Hashimoto M (2005) Identification of esterases expressed in Caco-2 cells and effects of their hydrolyzing activity in predicting human intestinal absorption. *Drug Metab Disp* **33**: 1185-1190.

Imai T, Taketani M, Shii M, Hosokawa M, Chiba K (2006) Substrate specificity of carboxylesterase isozymes and their contribution to hydrolase activity in human liver and small intestine. *Drug Metab Disp* **34**: 1734-1741.

Kamendulis LM, Brzezinski MR, Pindel EV, Bosron WF, Dean RA (1996) Metabolism of cocaine and heroin is catalyzed by the same human liver carboxylesterases. *J Pharmacol Exp Ther* **279**: 713-717.

Kühl PW (1994) Excess-substrate inhibition in enzymology and high-dose inhibition in pharmacology: a reinterpretation. *Biochem J* **298**: 171-180.

Kurihara A, Hagihara K, Kazui M, Ozeki T, Farid NA, Ikeda T (2005) In Vitro Metabolism of Antiplatelet Agent Clopidogrel: Cytochrome P450 Isoforms Responsible for Two Oxidation Steps Involved in the Active Metabolite Formation. *Drug Metab Rev* **37 (Suppl 2)**: 99.

Niitsu Y, Jakubowski JA, Sugidachi A, and Asai F (2005) Pharmacology of CS-747 (prasugrel, LY640315), a novel, potent antiplatelet agent with in vivo P2Y12 receptor antagonist activity. *Semin Thromb Hemost* **31**: 184-194.

Paine MF, Hart HL, Ludington SS, Haining RL, Rettie AE, Zeldin DC (2006) The Human Intestinal Cytochrome P450 "Pie". *Drug Metab Disp* **34**: 880-886.

Pindel EV, Kedishvili NY, Abraham TL, Brzezinski MR, Zhang J, Dean RA, Bosron WF (1997) Purification and cloning of a broad substrate specificity human liver carboxylesterase that catalyzes the hydrolysis of cocaine and heroin. *J Biol Chem* **272**: 14769-14775.

Rehmel JL, Eckstein JA, Farid NA, Heim JB, Kasper SC, Kurihara A, Wrighton SA, and Ring BJ (2006) Interactions of two major metabolites of prasugrel, a thienopyridine antiplatelet agent, with the cytochromes P450. *Drug Metab Disp* **34**: 600-607.

Sanghani SP, Quinney SK, Fredenburg TB, Davis WI, Murry DJ, Bosron WF (2004) Hydrolysis of irinotecan and its oxidative metabolites, 7-ethyl-10-[4-N-(5-aminopentanoic acid)-1-piperidino] carbonyloxycamptothecin and 7-ethyl-10-[4-(1-piperidino)-1-amino]-carbonyloxycamptothecin, by human carboxylesterases CES1A1, CES2, and a newly expressed carboxylesterase isoenzyme, CES3. *Drug Metab Disp* **32**: 505-511.

Satoh T, Hosokawa M (1998) The mammalian carboxylesterases: from molecules to functions. *Annu Rev Pharmacol Toxicol* **38**: 257-288.

Satoh T, Taylor P, Bosron WF, Sanghani SP, Hosokawa M, La Du BN (2002) Current progress on esterases: from molecular structure to function. *Drug Metab Disp* **30**: 488-493.

Sugidachi A, Ogawa T, Kurihara A, Hagihara K, Jakubowski JA, Hashimoto M, Niitsu Y, Asai F (2007) The greater in vivo antiplatelet effects of prasugrel as compared to clopidogrel reflect more efficient generation of its active metabolite with similar antiplatelet activity to that of clopidogrel's active metabolite. *J Thromb Haemost* **5**: 1545-1551.

Taketani M, Shii M, Ohura K, Ninomiya S, Imai T (2007) Carboxylesterase in the liver and small intestine of experimental animals and human. *Life Sci* **81**: 924-932.

Tang M, Mukundan M, Yang J, Charpentier N, LeCluyse EL, Black C, Yang D, Shi D, and Yan B (2006) Antiplatelet Agents Aspirin and Clopidogrel Are Hydrolyzed by Distinct Carboxylesterases, and Clopidogrel Is Transesterificated in the Presence of Ethyl Alcohol. *J Pharmacol Exp Ther* **319**: 1467-1476.

Wadkins RM, Morton CL, Weeks JK, Oliver L, Wierdl M, Danks MK, Potter PM (2001) Structural constraints affect the metabolism of 7-ethyl-10-[4-(1-piperidino)-1-piperidino]carbonyloxycamptothecin (CPT-11) by carboxylesterases. *Mol Pharmacol* **60**: 355-362.

Williams ET, Ehsani ME, Wang X, Wang H, Qian YW, Wrighton SA, Perkins EJ (2008) Effect of Buffer Components and Carrier Solvents on In Vitro Activity of Recombinant Human Carboxylesterases. *J Pharmacol Toxicol Methods*. **57**:138-144.

Williams JA, Ring BJ, Cantrell VE, Jones DR, Eckstein J, Ruterbories K, Hamman MA, Hall SD, Wrighton SA (2002) Comparative metabolic capabilities of CYP3A4, CYP3A5, and CYP3A7. *Drug Metab Disp* **30**: 883-891.

Figure 1 – The metabolic pathway of prasugrel leading to its active metabolite.

Figure 2 – The kinetics plots for the hydrolysis of prasugrel by hCE1 (A) and hCE2 (B). The points with the error bars represent the average and standard error, while the lines represent the best model fit of their respective kinetic models. (A) For hCE1, the curve is standard Michaelis-Menten kinetics. (B) For hCE2, data up to 40.5 μM were fit to the Hill equation, while the data 27.4 μM and above were fit to a standard IC_{50} model. The inset shows the sigmoidicity of the Hill kinetics.

Figure 3 – Cumulative amounts of prasugrel (solid line) and R-95913 (dotted line) in the donor and receiver wells for apical to basolateral (A and B, respectively) and basolateral to apical (C and D, respectively) experiments using a Caco-2 monolayer. Graphs are displayed as the average with the error bars representing the standard error.

Figure 1

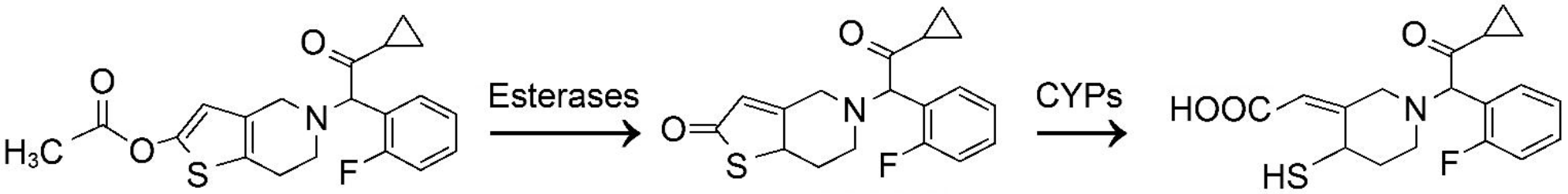

Prasugrel R-95913 R-138727

Figure 2

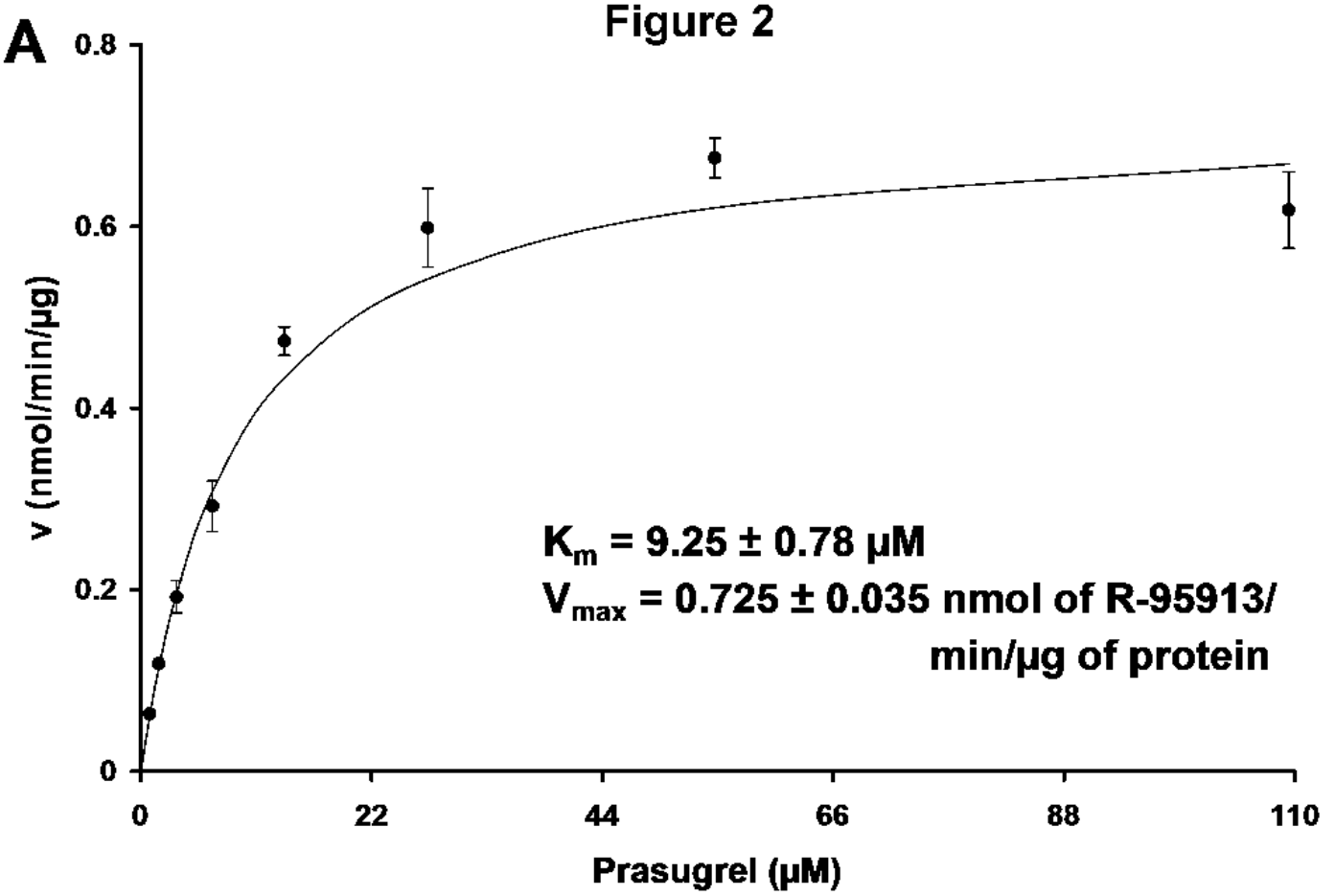
A
v (nmol/min/µg)
0.8
0.6
0.4
0.2
0
0
22
44
66
88
110
Prasugrel (µM)
K_m = 9.25 ± 0.78 µM
V_{max} = 0.725 ± 0.035 nmol of R-95913/ min/µg of protein

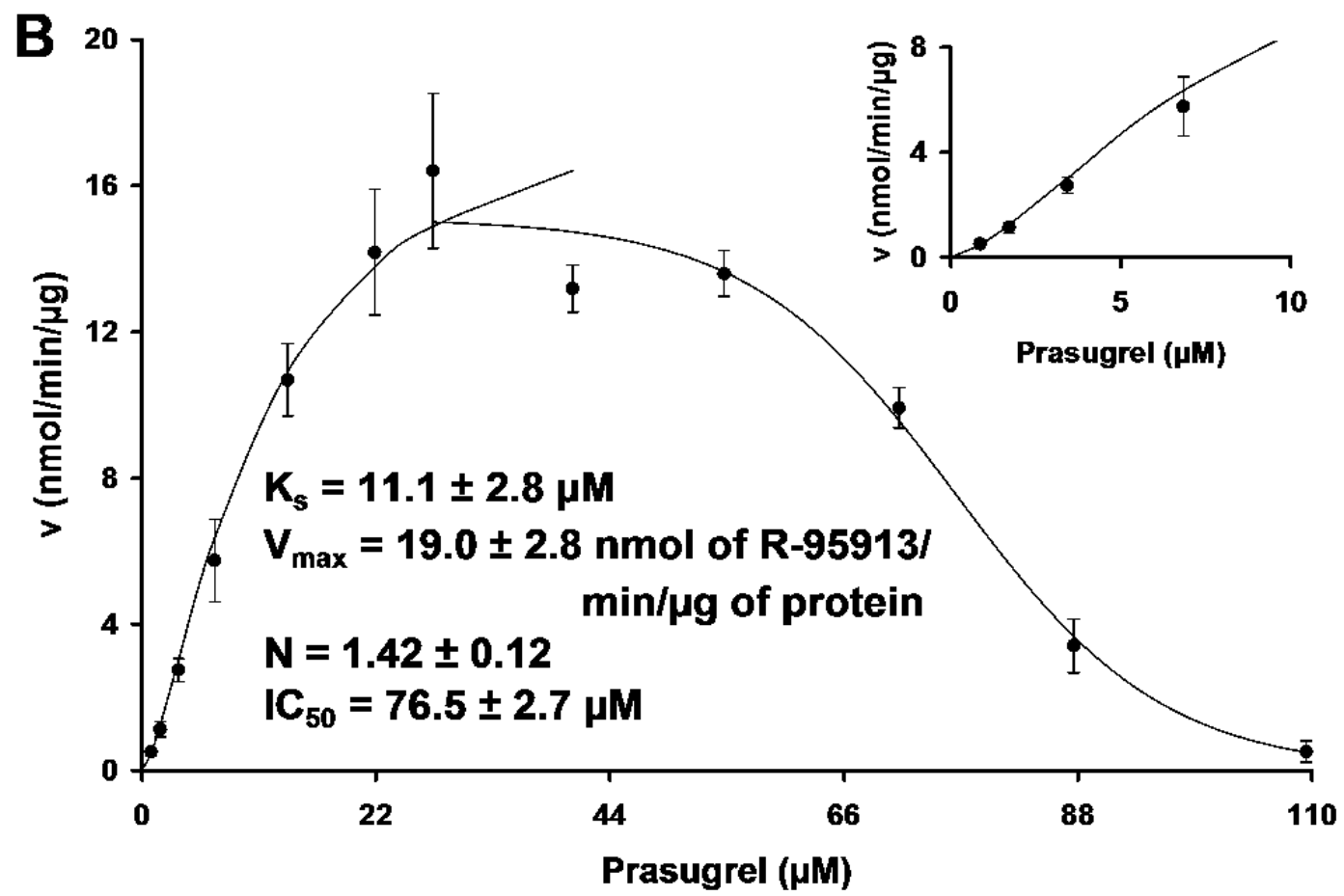
B
v (nmol/min/µg)
20
16
12
8
4
0
0
22
44
66
88
110
Prasugrel (µM)
K_s = 11.1 ± 2.8 µM
V_{max} = 19.0 ± 2.8 nmol of R-95913/ min/µg of protein
N = 1.42 ± 0.12
IC_{50} = 76.5 ± 2.7 µM
v (nmol/min/µg)
8
4
0
0
5
10
Prasugrel (µM)

Figure 3

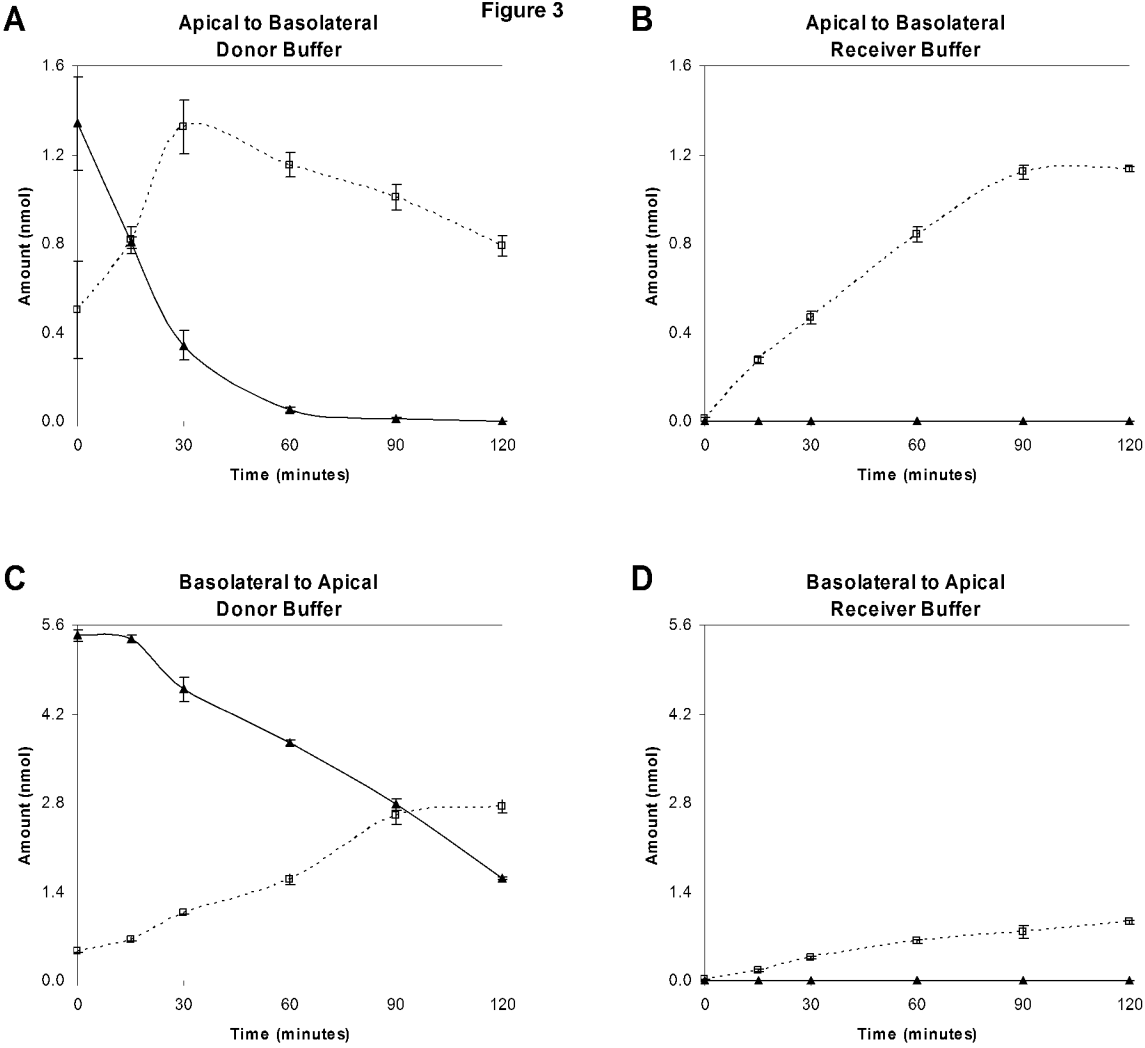
A
Apical to Basolateral
Donor Buffer
Amount (nmol)
Time (minutes)
B
Apical to Basolateral
Receiver Buffer
Amount (nmol)
Time (minutes)
C
Basolateral to Apical
Donor Buffer
Amount (nmol)
Time (minutes)
D
Basolateral to Apical
Receiver Buffer
Amount (nmol)
Time (minutes)